Fujimoto *Journal of Wood Science* (2023) 69:3
https://doi.org/10.1186/s10086-023-02078-1

Journal of Wood Science

ORIGINAL ARTICLE

Open Access

# Detecting the changes of wood properties with respect to elapsed years since wood formation by the eigenvalue distribution of near infrared spectral matrices

Takaaki Fujimoto*

## Abstract

The effects of aging on wood properties are usually evaluated based on cambial age, with the assumption that the properties do not change once the wood has formed. This study examined changes in wood properties with the number of years elapsed since wood formation. Near-infrared (NIR) spectra were acquired from various positions of 20 sample trees, and changes in the spectra were examined with respect to elapsed years. We considered changes in multiple traits inclusively, rather than individually, using the distribution of eigenvalues calculated from NIR spectral matrices. The diffusion of eigenvalues with an increase in elapsed years followed Dyson's Brownian motion. The gradual increase in the first eigenvalue, which is equivalent to the Helmholtz-free energy, indicates that the xylem in the heartwood changes to a more ordered physical state over time. The variations in Shannon entropy and density matrix with elapsed years revealed the irreversibility of the aging process. The proposed method is independent of a specific coordinate system and can, therefore, be applied using a wide variety of information other than that obtained from NIR spectra.

**Keywords** Dyson's Brownian motion, Fokker–Planck equation, Helmholtz-free energy, Entropy, Irreversible process

## Introduction

Trees grow in diameter through cell division of the vascular cambium, a sheath of meristematic cells situated between the secondary xylem and phloem [1]. In general, the properties of successive layers of xylem formed every year vary depending on tree age [2]. For instance, the wood density of hinoki cypress (*Chamaecyparis obtusa*) gradually decreases with age [3]. In other words, the wood density near the center of the stem is higher than that near the bark. The variation pattern of wood properties with respect to tree age has been studied intensively for several species, and has led to the concept of juvenile and mature wood [4]. As juvenile wood differs from mature wood and is undesirable for some products, timber industries should carefully consider the type of wood they use.

The effects of aging on wood properties are normally evaluated using cambial age [3]. Wood properties are measured at each growth ring, and their variations are expressed as a function of the ring number counted from the pith. These variations primarily arise from the effects of physiological aging, that is, the maturation of cambial cells. In this case, it is implicitly assumed that wood properties do not change once the wood forms. However, this assumption should be carefully considered. For instance, the first ring at the base of a 100-year-old tree endures various phenomena for several years, such as successive loads generated by the weight of the tree and growth stress. Therefore, it is expected that wood

*Correspondence:
Takaaki Fujimoto
tafujimoto@tottori-u.ac.jp
Faculty of Agriculture, Tottori University, Tottori 680-8553, Japan

properties would change during this period. Talbert and Jett (1981) found that juvenile wood of older loblolly pine (*Pinus taeda*) trees had a considerably higher specific gravity than that of juvenile wood of young trees, even after resin extraction [5]. Tsutsumi and Fujimoto (2016) also suggested that the extractive content of heartwood in Japanese oak (*Quercus crispula*) can change without physiological activities [6]. However, only a few studies have been conducted to evaluate changes in wood properties in accordance with the years elapsed since wood formation.

After a certain age, trees form heartwood, where the protoplasm of the living cells in the xylem dies [7]. As the xylem in heartwood loses its physiological activities entirely, changes in wood properties that occur after the formation of heartwood should be considered an anti-physiological phenomenon. Studies on archaeological wood help understand these phenomena [8]. Kohara (1958) reported that the columns and beams used in the five-story pagoda of Horyuji Temple, the world's oldest wooden architecture, showed greater stiffness, dimensional stability, and durability than those of modern wood [9]. These results are mainly derived from changes in the crystallinity of cellulose due to the long-term history of repeated heat and wetting–drying cycles [10–13]. These facts imply that the possible changes in wood properties in the heartwood of standing trees are essentially identical to those in archaeological wood.

Hinoki cypress is one of the most important commercial species in Japan, and its afforested area accounts for 25% of all forestry plantations in Japan [14]. Historically, hinoki has been used as a building material owing to its remarkable mechanical properties and durability. As mentioned above, the Horyuji Temple was built more than 1300 years ago, and hinoki was mainly used as its construction member [8]. However, wood resources have recently shifted from natural forests to plantation forests, and thus, wood properties of hinoki from plantation forests would vary with time. Accurately identifying the effects of aging on wood properties is necessary for adequate forest management and utilization of hinoki.

In a previous study, we discussed the effects of aging on wood properties from a physiological perspective, namely, the aging effects were considered as a function of cambial age [15]. The current study was conducted from an anti-physiological perspective, that is, the years elapsed since wood formation. Near-infrared (NIR) spectra were acquired from various positions on the tree, and changes in the spectra were examined with respect to the elapsed years (*EY*) calculated at each position. As wood properties vary in a complicated manner, we considered changes in multiple traits inclusively, rather than individually, using the distribution of eigenvalues calculated from NIR spectral matrices [16–19]. This approach allowed us to understand the variation in wood properties from a physical point of view.

## Materials and methods

### Sample materials

Twenty hinoki cypress trees grown in Tottori University Forest (35°160´N, 133°360´E; approximately 540 m elevation) were harvested in 2019 to ensure a wide variety of growth diameters. They were planted artificially for the experimental purpose. The mean and minimum to maximum values of tree height and diameter at breast height of sample trees were 19.5 m (16.6–23.8 m) and 27.5 cm (20.9–36.0 cm), respectively. Knot-free disks (5 cm thick) were cut from the base of the trees at 2 m intervals until they contained the heartwood. Based on the ring number at the base disk, the age of the sample trees was estimated to be 42 years. Radial strips (3 cm wide) that included the pith were cut from each sample disk along an arbitrary radial direction and left at room temperature until NIR experiments.

The *EY* at each growth ring were calculated as follows [6]: the cambial age (*CA*) was consistent with the number of growth rings counted from the center of the disk. If the disk at the $k^{\text{th}}$ position contains *M* growth rings, *M* years should have passed after the formation of the innermost ring. Consequently, the *EY* for each growth ring were calculated as follows:

$$EY = M_k - (CA_k - 1), k = 0, \cdots, K \tag{1}$$

where $M_k$ is the ring number containing the $k^{\text{th}}$ disk and $CA_k$ is the cambial age of the $k^{\text{th}}$ disk.

### NIR measurements

Diffuse reflectance spectra were acquired using a Fourier transform spectrophotometer (MATRIX-F; Bruker Optics Co., Tokyo, Japan) equipped with a fiber-optic probe (spot diameter ≈ 3.5 mm). The measurement spot was set across the latewood in the transverse section of the sample. NIR spectra were obtained at intervals of 8 $cm^{-1}$ over a wavenumber range of 10,000–4000 $cm^{-1}$. Zero-filling of two (corresponding to a spectral interval of 4 $cm^{-1}$) was applied. Sixty-four scans were collected to improve the signal-to-noise ratio and averaged into a single average spectrum. The measurements were conducted every two rings in two radial directions from the pith side to the outermost ring of the heartwood, and the mean of both values was used for the subsequent analysis.

The analyses focused on the wavenumber range of 9000–4500 $cm^{-1}$ to reduce computational complexity [16]. Before the spectral analyses, the original spectra were normalized. A total of 1,168 data points were

used as spectral variables across the spectral range (9000–4500 $cm^{-1}$).

### Data analysis

The data analysis procedure followed a previous study that examined the effects of aging on *CA* [15]. Briefly, the set of eigenvalues obtained from the spectral matrix at each growth ring plays a central role. Eigenvalue decomposition was applied to the variance–covariance matrix ($\boldsymbol{C}$) calculated from the spectral matrix $\boldsymbol{A}$ ($\boldsymbol{C}=\boldsymbol{A}^{\mathrm{T}}\boldsymbol{A}$):

$$\boldsymbol{C}\boldsymbol{u}_i = E_i\boldsymbol{u}_i, (i = 1, \cdots, n) \tag{2}$$

where $\boldsymbol{u}_i$ is an eigenvector, and $E_i$ is an eigenvalue associated with $\boldsymbol{u}_i$. According to the random matrix theory [20], the quadratic form ${u^{\mathrm{T}}}_i\boldsymbol{C}\boldsymbol{u}_i$ can be optimised as an energy function, termed Hamiltonian $H$ and determined by a variance–covariance matrix:

$$H(\boldsymbol{u}|\boldsymbol{C}) \equiv \boldsymbol{u}_i^{\mathrm{T}}\boldsymbol{C}\boldsymbol{u}_i \tag{3}$$

The superscript T indicates the transposed matrix. Once $H=\{E_1, E_2, \ldots, E_n\}$ is defined, the distribution function $Z$ can be calculated as [21, 22]

$$Z = \sum_{i=1}^{n} \exp(-\beta E_i), \tag{4}$$

where $\beta$ is the inverse temperature defined as $(kT)^{-1}$ ($k$ is the Boltzmann constant and $T$ is the absolute temperature). The distribution function $Z$ provides thermodynamic functions, such as the Helmholtz-free energy and entropy, and we discuss the organization and randomness of wood with *EY* based on the time evolution of these thermodynamic functions. These calculations were performed using the standard functions of R version 4.0.4.

## Results and discussion

### Variation of NIR spectra

The variation in the NIR spectra with respect to the *EY* is shown in Fig. 1a. As the original spectra did not show clear tendencies with *EY*, we processed them as a second derivative treatment. As a result, the absorption intensity exhibited characteristic changes in specific bands. For instance, a gradual decrease in the absorption over time was observed in the peaks at 5848 $cm^{-1}$, which were assigned to the first overtone of the C–H stretching mode of furanose/pyranose owing to hemicellulose [23]. This result was consistent with those of previous reports about the age dependency of hemicellulose content [11, 24].

The variation pattern of wood components with *EY* was not so obvious, although the second derivative spectra detected a successive decrease in hemicellulose. Moreover, it is insufficient to consider the changes in each variable individually as changes in one property induce changes in other properties. Hence, we did not consider the spectral variation as an individual variable (i.e., wavenumber), but rather as a whole for the physical system with multiple degrees of freedom [16]. This idea is closely related to statistical mechanics. The basic idea of statistical mechanics is that instead of considering a

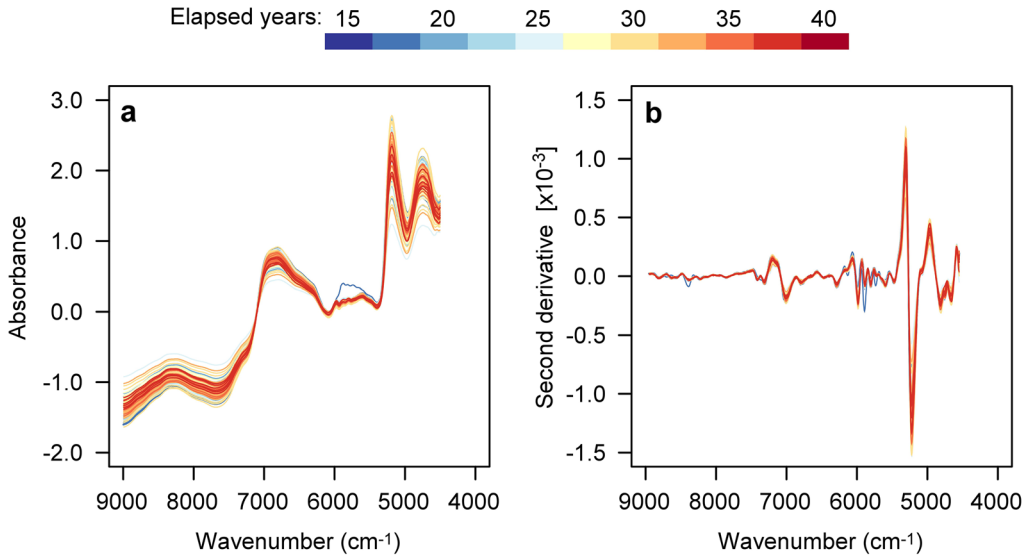


**Fig. 1** Variation of (**a**) the diffuse reflectance near-infrared (NIR) spectra and (**b**) their second derivative spectra with respect to the elapsed years since wood formation in hinoki cypress (*Chamaecyparis obtusa*). The colors of the lines change from blue to red with an increase in elapsed years

single dynamic system, we considered a collection of systems is considered that correspond to the same Hamiltonian, that is, a statistical ensemble [25, 26]. Herein, we assumed that the spectral variables were microscopic elements comprising the wood system. In other words, the NIR spectral matrix from an ensemble of wood samples could be identified with a point cloud in the *n*-dimensional phase space [27]. Thus, spectral variables serve as generalized coordinates in analytical mechanics [28, 29].

#### Changes of the eigenvalue distribution

As the NIR spectral matrix represents the variation in the ensemble of wood samples, the distribution of the eigenvalues calculated from the matrix should provide inclusive information of the ensemble. Moreover, the characteristic equation to solve the eigenvalue problem is invariant with respect to changes in the basis [30]. Therefore, the set of eigenvalues reveals the intrinsic variation of the wood ensemble. The distributions of eigenvalues ($E_i$) for representative *EY* are shown in Fig. 2. The eigenvalues in older *EY* were widely distributed compared to those in younger *EY*, indicating that the NIR spectral matrix varied in a more orderly manner as the *EY* increased. This is consistent with a previous study in which eigenvalues were widely distributed with cambial age [15].

As mentioned above, the set of eigenvalues represents the energy state of the system in the context of physics [20, 31, 32]. Therefore, changes in wood over time can be analyzed from the perspective of thermodynamics and statistical mechanics [21, 33]. Kabashima and Takahashi (2012) showed that the first eigenvalue $E_1$ of the variance–covariance matrix can be evaluated using the Helmholtz-free energy ($F$) in the limits of $\beta \to \infty$ [34]:

$$E_1 = 2 \lim_{\beta \to \infty} F(\beta | \boldsymbol{C}), \tag{5}$$

where $F$ is defined as a function of $\beta$ conditioned by the matrix $\boldsymbol{C}$, that is, $F(\beta|\boldsymbol{C}) = -\beta^{-1}\log Z(\beta|\boldsymbol{C})$. Figure 3a shows the trajectory of some representative eigenvalues with respect to *EY*. Consistent with the results shown in Fig. 2, the eigenvalues diffused without intersecting with each other. A clear increase in the first eigenvalue, which is equivalent to the Helmholtz-free energy, suggests that the xylem in heartwood changes to a more ordered physical state with an increase in *EY*. Based on the aforementioned suggestion, we confirmed the equivalence between the xylem in the heartwood of the standing tree and the archaeological wood. The superior mechanical properties and dimensional stability of archaeological wood are largely due to changes in the crystallinity of cellulose, that is, the regularity of its molecular configuration. Although many other properties also vary simultaneously with the mechanical properties and changes in dimensional stability, the diffusion of eigenvalues indicates that these complex variations represent the progress of the organization of the xylem tissue. As the diffusion of eigenvalues was also observed with an increase in *CA* [15], the phenomena should progress in both physiological and anti-physiological aging processes.

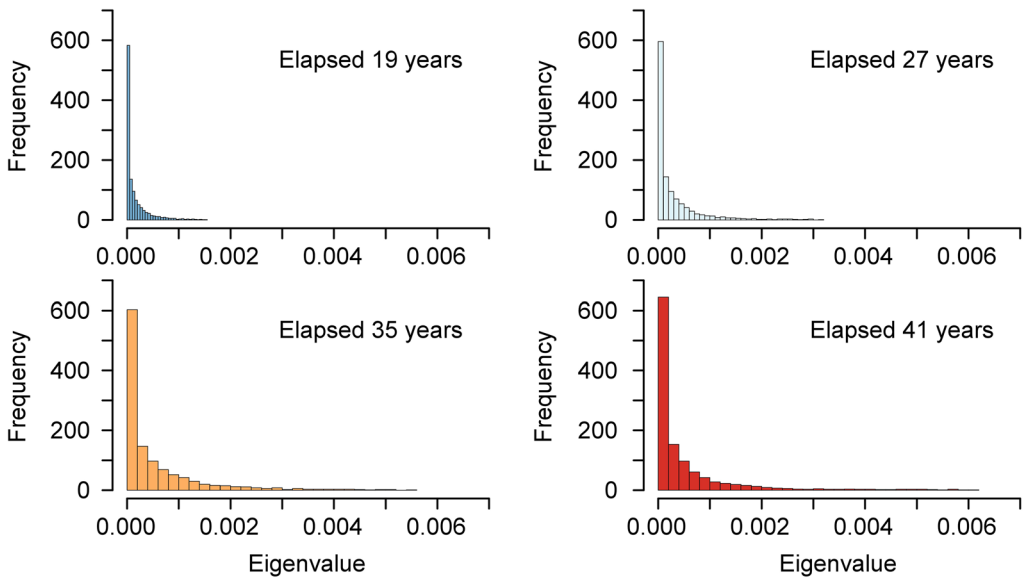


**Fig. 2** Distributions of eigenvalues at representative elapsed years

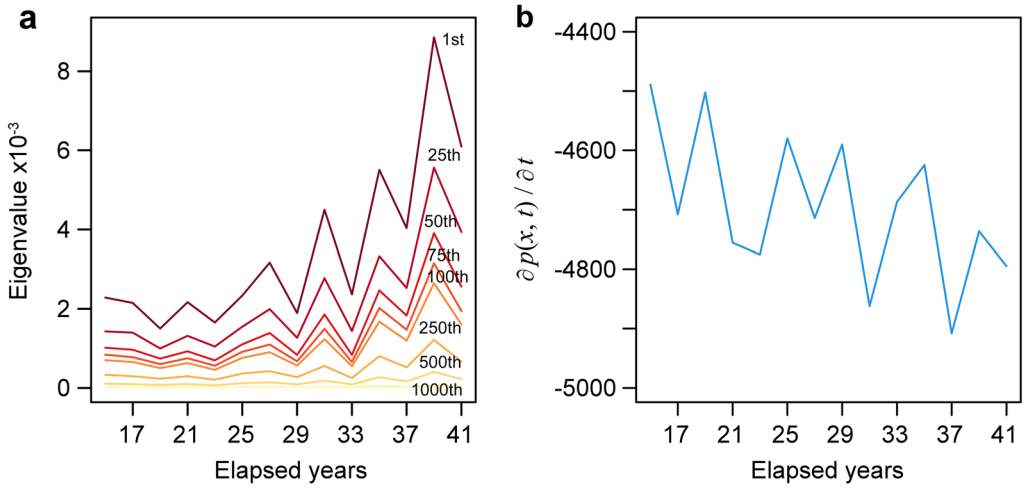


**Fig. 3** **a** Trajectory of the representative eigenvalues with elapsed years. **b** Differential of the probability density of the eigenvalues with respect to elapsed years. The number in (**a**) indicate the order of the eigenvalues

An $n \times n$ Hermitian matrix has $n$ eigenvalues that move along the real axis, and the stochastic process of the eigenvalues is called Dyson's Brownian motion [35]. Although the variance–covariance matrix is a real-symmetric, we discuss the time evolution of the eigenvalue distribution with respect to *EY* using the Dyson model. The stochastic dynamics of the eigenvalues $\{E_1, E_2, \ldots, E_n\}$ of the matrix are described as follows:

$$dE_i = dB_i + \sum_{\substack{1 \le j \le n \\ j \ne i}} \frac{dt}{E_i - E_j}, \quad 1 \le i \le n, \tag{6}$$

where $B_i$ $(1 \le i \le n)$ represents independent one-dimensional Brownian motions [33, 35]. From Eq. (6), the probability density of the eigenvalues, $p = p(E_1, \cdots, E_n, t)$, satisfies the Fokker–Planck equation [36]:

$$\frac{\partial}{\partial t} p = \sum_{i=1}^{n} \sum_{j \ne 1} \frac{1}{E_i - E_j} \frac{\partial p}{\partial E_i} + \frac{1}{2} \sum_{i=1}^{n} \frac{\partial^2 p}{\partial E_i^2} \tag{7}$$

The trajectory of the differential of $p$ with respect to the *EY* was calculated using Eq. (7), as shown in Fig. 3b. The differential coefficient of $p$ increased negatively with *EY*. It remains unclear why the opposite result was found in the case of cambial aging [15]. However, the complicated aging process can be understood if we solve the stochastic differential equation (Eq. 7) representing the motion of the eigenvalues, which contains all the variations generated by various wood properties. Moreover, it is important to note that the current results did not represent the behavior of individual trees, but that of a statistical ensemble with a large number of elements [20]. Hence, the trajectory of the Fokker–Planck equation should exhibit highly universal behavior based on the law of large numbers [37].

#### Randomness and irreversibility of the aging process

Here, we considered the changes in wood properties with respect to the elapsed time from the viewpoint of the randomness of the physical system. Using the distribution function $Z$ (Eq. 4) as a normalization factor, the probability that the system of interest could occupy the energy eigenstate $E_i$ can be expressed as

$$p_i^{\mathrm{can}} = \frac{1}{Z} \exp(-\beta E_i) \tag{8}$$

$p_i^{\mathrm{can}}$ is equivalent to the canonical distribution in statistical physics [25]. Let $\beta$ be a constant. The distribution of $p_i^{\mathrm{can}}$ corresponding to each energy eigenstate in the representative *EY* is shown in Fig. 4a. The $p_i^{\mathrm{can}}$ of the younger *EY* had flatter distributions compared with those of the older *EY*, indicating that the probability distribution of the eigenstate of energy is biased with an increase in *EY*. We can then calculate the Shannon entropy ($S$) as a function of $p_i^{\mathrm{can}}$ [21]:

$$S = -\sum_{i=1}^{N} p_i^{\mathrm{can}} \log p_i^{\mathrm{can}} \tag{9}$$

Both $Z$ and $p_i^{\mathrm{can}}$ depend on the inverse temperature $\beta$ [see Eqs. (4) and (8)]. The entropy $S$ can be evaluated for each $\beta$. Figure 4b shows the change in entropy *EY* for various $\beta$ conditions. The curves of $S$ changed from red to yellow (from top to bottom) as the inverse temperature increased. The domain of $\beta$ was set from 1 to 100,000

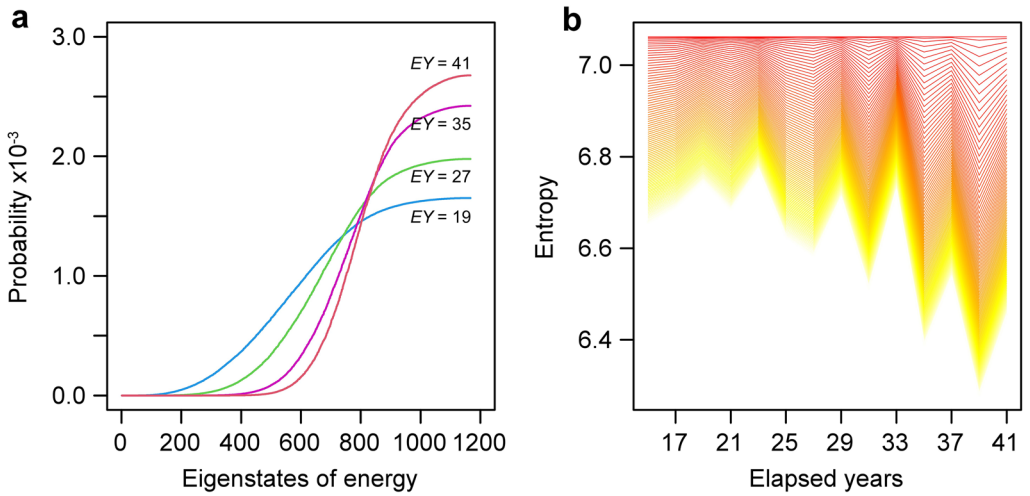


**Fig. 4** **a** Probability distributions corresponding to each energy eigenstate at representative elapsed years. **b** Changes of entropy with the elapsed years for various inverse temperature conditions. The colors of the lines change from red to yellow as the inverse temperature increases

to enable entropy calculation. The entropy gradually decreased with *EY* at almost every inverse temperature. These results are consistent with the trend of the Helmholtz-free energy, where the xylem at younger *EY* is in a random state as a physical system, and that at older *EY* is in a more ordered state.

Suppose that the motion of a wood system of m points in *n*-dimensional space is expressed by Hamilton's equations:

$$\frac{dq_i}{dt} = \frac{\partial H}{\partial p_i}, \frac{dp_i}{dt} = \frac{\partial H}{\partial q_i}, \tag{10}$$

where $\boldsymbol{q} = (q_1, \cdots, q_n)$ represents the generalised coordinates and $\boldsymbol{p} = (p_1, \cdots, p_n)$ represents the momenta. A space of $2n$ dimensions spanned by $q_1$, ..., $q_n$, $p_1$, ..., $p_n$ is called the phase space. The point cloud, i.e., an ensemble of wood samples, can be described as a continuous fluid with a density of $\rho(q_1, \cdots, q_n, p_1, \cdots, p_n, t)$ in the phase space [29]. Based on the quantum mechanics [32], the density matrix can be calculated as

$$\rho = \sum_{i=1}^{n} \boldsymbol{u}_i^{\mathrm{T}} p_i^{\mathrm{can}} \boldsymbol{u}_i, \tag{11}$$

where $\boldsymbol{u}_i$ ($i = 1$, ..., $n$) is the eigenvector corresponding to eigenvalue $E_i$ (see Eq. 3). The time evolution of the density matrix is given by the Liouville–von Neumann equation [25]:

$$i\hbar \frac{\partial \rho}{\partial t} = [\rho, H], \tag{12}$$

where $i = \sqrt{-1}$ is imaginary unit, $\hbar$ is reduced Planck constant, $H$ is the diagonal matrix whose elements are eigenvalues calculated using Eq. (3), and the bracket [,] is the commutator defined by two operators $[A, B] = AB - BA$. This can be interpreted as a volume change of the fluid in the phase space. Liouville's theorem states that the fluid volume in the phase space is invariant if the system satisfies the law of conservation [29]. Thus, the density matrix $\rho$ is the first integral of Hamilton's Eq. (10), which is determined by the Hamiltonian $H$ (Eq. 3) if, and only if $[\rho, H] = 0$. The right-hand side of Eq. (12) was calculated for each *EY* and was a non-zero matrix. The matrix norms of commutator $[\rho, H]$ exhibited the same trend as the first eigenvalue (data not shown). The density matrix changed significantly with *EY* and did not conserve its volume. As energy invariance refers to the symmetry of a process from a geometrical perspective (Noether's theorem [25]), the results infer that the aging phenomenon with respect to the elapsed years is an irreversible process, and symmetry breakage during the process becomes more pronounced with the elapsed years. A previous study found similar irreversibility in the aging phenomenon with respect to the *CA* and proposed that wood with the same properties is never renewable [15]. The current study supports this proposition as wood cannot be restored to its original state through the anti-physiological aging process.

## Conclusions

The effects of aging on wood properties can be considered from two perspectives: physiological and anti-physiological. This study focused on the anti-physiological aging in which the xylem in heartwood changes with the number of years elapsed since wood formation. Changes in wood properties in heartwood of standing trees were analogous to those in archaeological wood, where the

diffusion of eigenvalues indicated that the xylem in heartwood changed to a more ordered physical state with an increase in *EY*. It should be noted that as the aging process is irreversible, wood with the same properties is never renewable. The results of this study have implications for forest ecology and management.

**Abbreviations**

| | |
|---|---|
| CA | Cambial age |
| EY | Elapsed years |
| NIR | Near infra-red |

**Acknowledgements**
The author acknowledges Professor Satoru Tsuchikawa of Nagoya University for assisting with NIR measurements. The author is grateful to Mr. Shogo Fukutomi and Ms. Asami Yoneda of the Tottori University Forest for harvesting the sample trees. This work was supported by JSPS KAKENHI (Grant Number: JP21K05709). The author would like to thank Editage (www.editage.com) for English language editing.

**Author contributions**
Takaaki Fujimoto: investigation, formal analysis, resources, conceptualization, methodology, writing, review, and editing. The author read and approved the final manuscript.

**Funding**
This work was supported by JSPS KAKENHI (Grant Number: JP21K05709).

**Availability of data and materials**
Not applicable.

## Declarations

**Competing interests**
The authors declared no potential conflicts of interest with respect to the research, authorship, and/or publication of this article.

Received: 13 September 2022 Accepted: 26 December 2022
Published online: 12 January 2023

**References**

1. Panshin AJ, de Zeeuw C (1970) Textbook of Wood Technology, 3rd edn. McGraw-Hill, New York
2. Zobel BJ, van Buijtenen JP (1989) Wood variation—its causes and control. Springer, Berlin
3. Kimura J, Fujimoto T (2014) Modeling the effects of growth rate on the intra-tree variation in basic density in hinoki cypress (*Chamaecyparis obtusa*). J Wood Sci 60:305–312. https://doi.org/10.1007/s10086-014-1416-0
4. Zobel BJ, Sprague JR (1998) Juvenile Wood in Forest Trees. Springer, Berlin
5. Talbert JT, Jett JB (1981) Regional specific gravity values for plantation grown loblolly pine in the southeastern United States. For Sci 27:801–807
6. Tsutsumi H, Fujimoto T (2016) Effects of aging on the extractive contents of Japanese oak (*Quercus crispula*) heartwood as evaluating based on cambial age and elapsed time since wood formation. J Forest Biomass Utilization Soc 11:19–25
7. Hillis WE (1987) Heartwood and Tree Exudates. Springer-Verlag, Berlin
8. Yokoyama M, Gril J, Matsuo M, Yano H, Sugiyama J, Clair B, Kubodera S, Mistutani T, Sakamoto M, Ozaki H, Imamura M, Kawai S (2009) Mechanical characteristics of aged Hinoki wood from Japanese historical buildings. C R Phys 10:601–611. https://doi.org/10.1016/j.crhy.2009.08.009
9. Kohara J (1958) Study on the old timber. Res Rep Faculty Eng Chiba Univ 9(15):1–55
10. Kohara J, Okamoto H (1956) Study on the old timber—Changes in chemical component. Mokuzai Gakkaishi 2:191–195
11. Yonenobu H, Tsuchikawa S (2008) Near-infrared spectroscopic comparison of antique and modern wood. Appl Spectrosc 57:1451–1453. https://doi.org/10.1366/000370203322554635
12. Tsuchikawa S, Yonenobu H, Siesler HW (2005) Near-infrared spectroscopic observation of the ageing process in archaeological wood using a deuterium exchange method. Analyst 130:379–384. https://doi.org/10.1039/b412759e
13. Inagaki T, Yonenobu H, Tsuchikawa S (2008) Near-infrared spectroscopic monitoring of the water adsorption/desorption process in modern and archaeological wood. Appl Spectrosc 62:860–865. https://doi.org/10.1366/000370208785284312
14. Forestry Agency (2020) Annual report on trends in forests and forestry, fiscal year 2020 (summary). https://www.rinya.maff.go.jp/j/kikaku/hakusyo/R2hakusyo/attach/pdf/index-4.pdf. Accessed 27 Dec 2022
15. Fujimoto T (2022) Evaluation of the age dependent variation of wood properties based on the eigenvalue distribution of near infrared spectral matrices. Chemometr Intell Lab Syst. https://doi.org/10.1016/j.chemolab.2022.104576
16. Fujimoto T (2019) Evaluation of wood variation based on the eigenvalue distribution of near infrared spectral matrix. J Near Infrared Spectrosc 27:175–180. https://doi.org/10.1177/0967033518812894
17. Fujimoto T (2021) Evaluation of stress relaxation process of wood based on the eigenvalue distribution of near infrared spectra. Spectrochim Acta A Mol Biomol Spectrosc. https://doi.org/10.1016/j.saa.2020.119197
18. Tsutsumi H, Haga H, Fujimoto T (2020) Variation in wood shrinkage evaluated by the eigenvalue distribution of the near infrared spectral matrix. Vib Spectrosc. https://doi.org/10.1016/j.vibspec.2020.103091
19. Tsutsumi H, Haga H, Fujimoto T (2020) Energetics of the distribution of cell wall in wood based on an eigenvalue analysis. J Wood Sci 66:58. https://doi.org/10.1186/s10086-020-01908-w
20. Mehta ML (2004) Random matrices, 3rd edn. Elsevier Ltd, London
21. Helrich CS (2009) Modern Thermodynamics with Statistical Mechanics. Springer-Verlag, Berlin
22. Landau DP, Binder K (2015) A guide to Monte Carlo simulations in statistical physics, 4th edn. Cambridge University Press, Cambridge
23. Schwanninger M, Rodrigues JC, Fackler K (2011) A review of band assignments in near infrared spectra of wood and wood components. J Near Infrared Spectrosc 19:287–308. https://doi.org/10.1255/jnirs.955
24. Takei T, Hamajima M, Kamba N (1997) Fourier transform infrared spectroscopic analysis of the degradation of structural lumber in Horyu-ji temple. Mokuzai Gakkaishi 43:285–294
25. Toda M, Kubo R, Saito N (1998) Statistical physics I Equilibrium Statistical Mechanics, Third corrected printing. Springer-Verlag, Berlin
26. Schwabl F (2006) Statistical Mechanics, 2nd edn. Springer-Verlag, Berlin
27. Prigogine I (1980) From Being to Becoming – Time and Complexity in the Physical Sciences. W H Freeman and Company, San Francisco
28. Lanczos C (1970) The Variational Principles of Mechanics, 4th edn. Dover Publications Inc, New York
29. Arnold VI (1989) Mathematical Methods of Classical Mechanics, 2nd edn. Springer Science+Business Media Inc, New York
30. Lang S (1987) Linear Algebra, 3rd edn. Springer Science+Business Media Inc, New York
31. Dyson FJ (1962) Statistical theory of the energy levels of complex systems I. J Math Phys 3:140–156. https://doi.org/10.1063/1.1703773
32. Schwabl F (2007) Quantum Mechanics, 4th edn. Springer-Verlag, Berlin
33. Kubo R, Toda M, Hashitsume N (1998) Statistical physics II Nonequilibrium Statistical Mechanics Third corrected printing. Springer-Verlag, Berlin
34. Kabashima Y, Takahashi H (2012) First eigenvalue/eigenvector in sparse random symmetric matrices: influences of degree fluctuation. J Phys A Math Theor. https://doi.org/10.1088/1751-8113/45/32/325001
35. Dyson FJ (1962) A Brownian-motion model for the eigenvalues of a random matrix. J Math Phys 3:1191–1198. https://doi.org/10.1063/1.1703862
36. Sasamoto T (2011) A note on a few processes related to Dyson's Brownian motion. RIMS Kôkyûroku Bessatsu B27:123–139
37. Sekimoto K (2010) Stochastic Energetics. Springer-Verlag, Berlin

## Publisher's Note